



Tailoring the structure and property of silicon-doped diamond-like carbon films by controlling the silicon content

Junjun Wang^{a,b}, Jibin Pu^a, Guangan Zhang^a, Liping Wang^{a,*}

^a State Key Laboratory of Solid Lubrication, Lanzhou Institute of Chemical Physics, Chinese Academy of Sciences, Lanzhou 730000, PR China

^b University of Chinese Academy of Sciences, Beijing 100039, PR China

ARTICLE INFO

Article history:

Received 24 April 2013

Accepted in revised form 26 July 2013

Available online 2 August 2013

Keywords:

Silicon-doped diamond-like carbon film
Hollow cathode plasma immersion ion
implantation method
Tribological property
Mechanical property

ABSTRACT

Diamond-like carbon (DLC) films have been extensively studied over the past decades due to their unique combination of properties; in particular, silicon-doped DLC (Si-DLC) films are of significant interest for tribological effects. But there are contradictory reports in the literature with regard to the effect of silicon content on the properties of DLC films. In this study, Si-DLC films were deposited by hollow cathode plasma immersion ion implantation (HCPIII) method, using mixtures of C₂H₂, Ar and diluted SiH₄ (SiH₄/Ar 10:90). The influences of Si addition on the surface morphology, structure, mechanical and tribological properties were investigated by a combination of surface analysis methods, nanomechanical and friction measurements. It was observed that addition of Si into DLC films lead to a decrease in the Raman band intensity ratio I_D/I_G. The root mean square values of Si-DLC films were increased along with the increase of Si concentration. Both the hardness and elastic modulus suffered degradation when the silicon concentration was low, but these properties recovered when Si concentration increased. The Si-DLC film with tensile stress and compressive stress can be obtained by choosing distinct contents of Si in the film. The coefficient of friction (COF) of Si-DLC films against GCr 15 steel ball under atmosphere firstly increased as the Si concentration increased up to 8.41 at.%, then COF of Si-DLC films decreased with a further increase of Si concentration. The mismatch in the bond length, the difference of the mechanical property and the alteration of the colliding particles' energy were determined to be the basis for the changes in these properties.

© 2013 Elsevier B.V. All rights reserved.

1. Introduction

Diamond-like carbon (DLC) films, an amorphous carbonaceous material composed of sp² carbon, sp³ carbon and hydrogen, have excellent properties such as low friction coefficient, high wear resistance, chemical inertness, high hardness and optical transparency. Because of these excellent properties, DLC films have attracted great attention for use in various applications such as electronic, optical and wear protection [1–4]. However, without transition layer or element doping, high intrinsic stress several gigapascals higher and mismatch in chemical bonding between the DLC films and the substrates often cause for poor adhesion. In addition, the thermal degradation caused by graphitization and hydrogen loss at higher temperature limit the working temperature of the films, the hardness of DLC film with hydrogen is lower than other hard carbon films, and their terminological properties strongly sensitive to the testing atmospheres [4–7].

Incorporation of other elements into the DLC films provides an effective way to improve the properties of the DLC films [7–12]. In particular, silicon-doped DLC (Si-DLC) films are of significant interest for tribological effects. They had a very low friction coefficient and possessed the

potential to improve wear performance in humid atmospheres and at higher temperatures. However, there are contradictory reports in the literature with regard to the effect of silicon content on the mechanical properties of DLC films. Lee etc. [13] showed that the mechanical properties of Si-DLC films changed significant when the silicon concentration was less than 5 at.%. In this concentration range, the harness, the residual stress and the elastic constants increased with increasing Si concentration. For higher concentration of Si, the mechanical properties showed saturated behaviors. Papakonstantinou etc. [14] observed that Si addition up to 20.2 at.% promoted the formation of sp³ bonding and reduced the hardness. Bendavid etc. [15] found that the DLC film without Si exhibited the higher hardness about 14GPa. However, as the Si content increased to about 4 at.%, the hardness value dropped to 12.4 GPa. For high Si content, the hardness saturated to value about 12 GPa. Recently, Fujimoto etc. [16] prepared Si-DLC films by dc pulse-plasma chemical vapor deposition. The results showed that an increase in Si lead to a decrease in hardness when the pulse voltage was – 2 kV. However, at a pulse voltage of – 5 kV, an increase in Si lead to a slight increase in hardness.

There are many methods of fabricating DLC films, magnetron sputtering [17], pulsed laser deposition [18], ion beam assisted deposition (IBAD) [19], plasma-assisted chemical vapor deposition (PECVD) [20] and plasma immersion ion implantation (PIII) method [21].

* Corresponding author. Tel./fax: +86 9364968080.
E-mail address: lpwang@licp.cas.cn (L. Wang).

Table 1
Deposition conditions for Si-DLC films.

Samples	Ar (sccm)	SiH ₄ (sccm)	C ₂ H ₂ (sccm)	Voltage (kV)	Duty cycle (%)	Thickness (μm)
1	100	0	100	−10	30	3.0
2	100	20	100	−10	30	3.4
3	100	50	100	−10	30	3.2
4	100	80	100	−10	30	3.2
5	100	100	100	−10	30	3.2

Compared with other synthesis methods, PIII method is a low-temperature process; thus, there is no need to consider base material softening, dimensional changes, and other problems caused by the increased temperature during film fabrication. In addition, this method can make DLC films with low residual stress and good adhesion to the substrate because the films are formed by simultaneous deposition with ion implantation [22]. For PIII method, there exist different methods for the generation of the plasma. In our previous work, a novel hollow cathode plasma immersion ion implantation (HCPIII) method was developed. This method takes advantage of plasma ion immersion and high density hollow cathode plasma generated between two parallel-plate electrodes plate, allowing decomposition of precursor and subsequent deposition of super-thick DLC-based films [23]. In this study, the objective is to investigate the effects of silicon incorporation on the microstructure, mechanical and tribological properties of DLC films prepared by HCPIII method.

2. Experimental

The substrates used for each deposition were stainless steels (30 mm × 20 mm × 1 mm) for tribological tests and (1 0 0) Si wafers (30 mm × 20 mm × 0.625 mm) for microscopic observations of film microstructures. Prior to deposition, the substrates were cleaned ultrasonically in ethanol and acetone baths in succession and then dried with nitrogen. The deposition experiments were carried out using a plane hollow cathode plasma-enhanced chemical vapor deposition system. The deposition system consists of a stainless steel vacuum chamber fitted with two parallel-plate electrodes. Prior to deposition, the surface of substrates was cleaned and etched to remove surface residual contaminants by introducing Ar gas into the chamber, the selection of parameters were listed in Table 1. After the argon plasma sputter cleaning of the substrate surface, silicon ions were implanted into the substrate from the silane (SiH₄) plasmas to produce the interfacial mixing layer of silicon and substrate materials. Then Si-DLC film deposited on substrate was carried out by introducing a mix gas of silicon and hydrocarbon precursor gas using the parameters listed in Table 1. Five coatings with varying Si contents were considered in this report.

The morphologies of as-prepared specimens were measured with scanning electron microscopy (SEM, JSM-5310 and JEOL) and atomic force microscopy (AFM, CSPM4000, Benyuan, China). The microstructure of the interface between the DLC film and the substrate was examined by high-resolution transmission electron microscopy (HRTEM, JE M-4000EX, JEOL) observations and fast Fourier transform (FFT) diffraction patterns in combination. Auger Electron spectroscopy (AES) is used to characterize the film–substrate interface composition. The composition of the film was determined by X-ray photoelectron spectroscopy (XPS). The XPS spectra were acquired employing a PHI-5700 with unmonochromatized Mg Ka radiation ($h\nu = 1253.6$ eV). The experimental resolution was 0.125 eV. Raman spectra were achieved using a Renishaw 2000 micro-Raman system operated at an argon laser wavelength of 514.5 nm and a 1800 line/nm grating. After measuring the bending of the coated substrate with a surface profilometer, the film internal stress was calculated by Stoney's equation. A calibrated Hysitron Triboindenter with a Berkovich indenter was employed to determine the film hardness (H) and Young's modulus (E). A maximum load of 10 mN was used in order to assure that the indentation depth was within the 10% of the film thickness. Six repeated measurements were made for each specimen. The tribological performances tested using a CSM tribometer with a reciprocating sliding configuration. The frequency was 5Hz, the sliding distance was 5 mm and the load was 5 N. The counterpart was hardened (HRC 60–62) GCr 15 steel ball with a diameter of 6 mm. All the tests were conducted at room temperature of about 24 ± 2 °C, and a relative humidity of 20%–30%. A non-contact 3D surface profiler (model MicroMAXTM, made by ADE Phase Shift, Tucson, AZ, USA) was used to capture 3D images on a wear track for measuring the wear volume. Three profilometry traces were taken on each wear surface to obtain wear depths and cross-sectional areas. The wear rate of the films was defined as the wear surface volume divided by the load and the total distance traveled by the counterface ball.

3. Results and discussion

Cross sections of DLC and Si-DLC films are dense and featureless. The thickness of all the films are controlled to about 3.2 μm, and the deposition rate is 3.2 μm/h. The microstructure and composition of the interface between the substrate and the DLC film are estimated by TEM and AES, respectively, as shown in Fig. 1(a) and (b). It is observed that an 11-nm interlayer containing Si, O and Fe is formed between the DLC film and the substrate, which may be due to high-energy ion implantation into the substrate and leads to substrate crystal structure damage. The observed O may attribute to the destruction of the oxide layer on the substrate surface by Si ion implantation. The diffuse cloudy FFT patterns of the DLC film indicate the absence of crystalline phases. The formatted translation layer probably decreases the mismatch

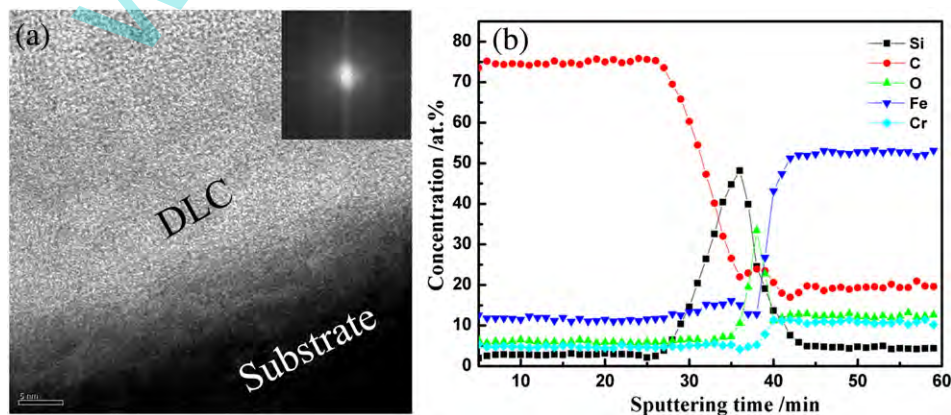


Fig. 1. (a) Cross-sectional TEM and (b) AES of interlayer between the DLC coating and the 304 stainless steel substrate.

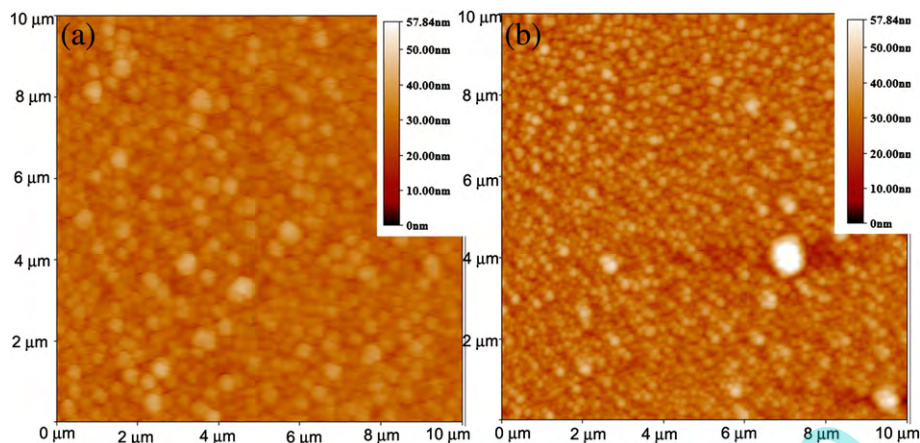


Fig. 2. Typical AFM images of DLC and Si-DLC films. (a) Pure DLC and (b) Si-DLC with 15 at.% Si.

between the film and the substrates, thereby reduces the interfacial stress and improving film adhesion [24].

AFM was employed to observe the topography and to measure the surface roughness of the samples. Typical AFM images of the pure DLC and Si-DLC films are shown in Fig. 2. It is seen that all the films have granular structure and the size of particles of DLC film is larger than that of Si-DLC film. The root-mean-squared roughness (RMS) of the samples versus the Si concentration is summarized in Fig. 3. The RMS of pure DLC films is 3.12 nm, which is lower than those of Si doped DLC films. The RMS of Si-DLC film range 4.90 to 6.02 nm with Si content from 7.14 at.% to 14.79 at.%.

Raman spectroscopy is one of the most common methods to probe amorphous carbon films due to its ability to distinguish bonding type and domain size. A typical Raman spectrum of DLC is composed of G and D bands, in which the G band centered approximately at 1555 cm^{-1} is due to the stretching vibrations of any pairs of sp^2 sites in chains or aromatic rings and the D band at approximately 1330 cm^{-1} comes from the breathing mode of those sp^2 sites only in aromatic rings. Fig. 4 shows a series of Raman spectra of the as-prepared DLC films with different Si contents. It is evident that all the films show typical characters of DLC. With increase in Si content, the Raman line shape changes from asymmetric to more symmetric. The D line and G line profiles are fitted by Lorentzian and BWF

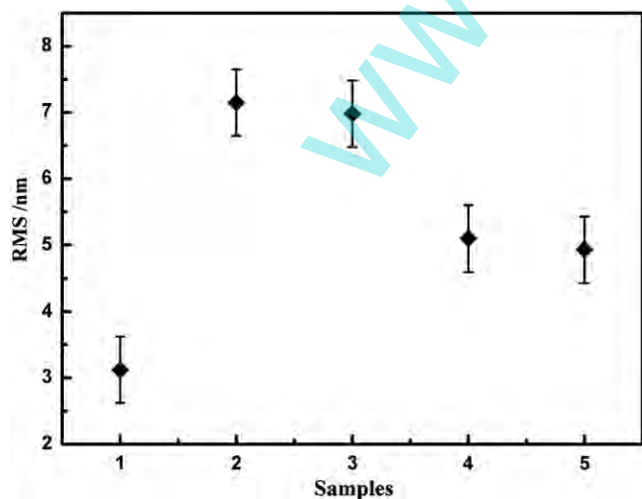


Fig. 3. RMS values of Si-DLC films with different Si content. Reported values and error bars represent averages and standard deviations, respectively, based on at least three different measurements on each of as-prepared films.

function, respectively [2,25,26]. The fitting results for the spectra, e.g., G peak position, G peak FWHM and the I_D/I_G , are shown in Figs. 5 and 6. It is clear that the G peak position shift from 1566 to 1484 cm^{-1} and G peak FWHM increases from 128 to 194 cm^{-1} with an increase in Si concentration from 0 to 14.79 at.%. The ratio I_D/I_G of the films decreased from about 1.16 for the Si-free DLC to 0.58 for the 14.79 at.% Si-DLC. The shift of the G band position to lower frequency can be partially attributed to a reduction in internal stress when silicon is introduced into the films because the longer de-strained bonds vibrate at lower frequency. For G peak full width at half maximum (FWHM) and I_D/I_G , they have been taken to be indicative of the sizes of the sp^2 islands inside the material [27]. The Si-free DLC have the largest I_D/I_G and smallest G peak FWHM, possibly indicating larger graphitic cluster sizes than the Si-DLC films, which have smaller I_D/I_G and larger G peak FWHM. Therefore, we can conclude that incorporation Si into DLC film reduce the size of Csp^2 clusters and create higher disorder in the DLC film.

Table 2 gives the Si, C and O at.% detected in the films by XPS analysis. It shows that the carbon, Si and O are detected in the surface of Si-DLC and only carbon and oxygen are presented in the surface of pure DLC films. The silicon concentration almost linearly increased with the SiH_4 flow ratio during the deposition. With the SiH_4 flow rate 100 sccm min^{-1} , the silicon concentration increase to 14.79 at.% and the carbon concentration drop to 74.49 at.%. Comparing to XPS data obtain from pure diamond with 1.4 eV and graphite with an FWHM 1.3 eV

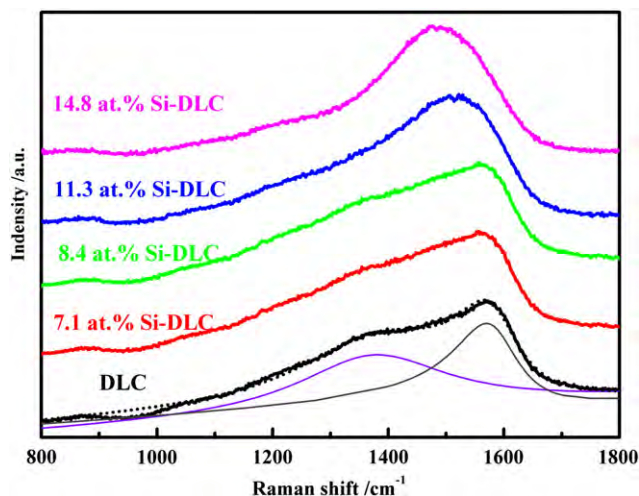


Fig. 4. Raman spectra of Si-DLC films with various Si content.

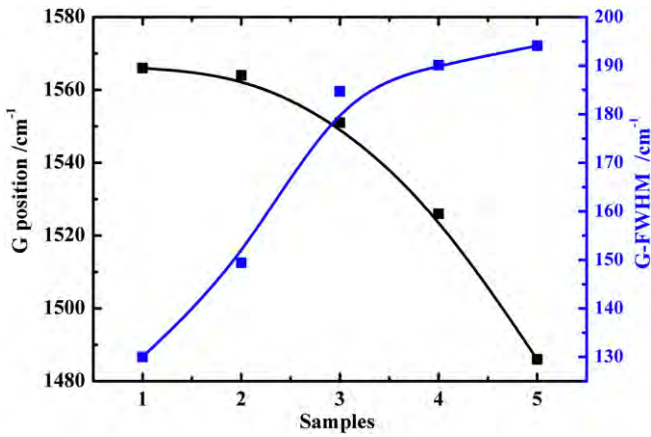


Fig. 5. Raman G peak position and G FWHM versus Si concentration.

[28], the C1s peaks obtain in this study are broad with an FWHM of 1.7 ± 0.1 eV. This results may duo to the possible presence of several bonding configurations for the C1s peak. Considering the presence of Si and O in the films, the C1s peak can be fit with four peaks representing four carbon bonding configurations. Four contributions are deconvoluted [19,29]: C-Si at 283.0 ± 0.12 eV, C = C at 284.3 ± 0.1 eV, C-C at 284.8 ± 0.1 eV and C-O at 286.4 ± 0.20 eV seen Table 1. The Si 2p features are fit with two peaks: one at about 100.5 eV and another at around 102.5 eV. The peak with a lower binding energy is consistent with the Si-C. The peak with a higher binding energy mostly rises from the presence of Si-O. All films contain an O1s peak locates at a binding energy of about 532 eV, which is assigned to C-O bonding. Parts a-c of Fig. 7 show deconvoluted C1s and Si 2p XPS peaks of the 14.7 at.% Si-DLC film. Absolute sp^3/sp^2 ratio cannot be calculated from XPS data. However, trend observed in XPS can provide useful information. Fig. 8 shows the fitted peak area as a function of Si concentration. From Fig. 8a, it can be see that pure DLC film contain the highest levels of C-C sp^2 bonding. The C-C sp^3 and Si-C bonding tend to increase with Si content. Meanwhile, it is clear that the Si-C and increase and Si-O decrease with Si concentration (Fig. 8b and c). Thus, adding a higher amount of Si, not only the amount of C-Si bond is increased but also the C-C sp^3 bonds, indicating the formation of amorphous diamond material. This results may be due to H₂ recombination energy release [30].

Fig. 9 shows the hardness values of the Si-DLC films as a function of Si concentration. Given that the maximum penetration depth is less

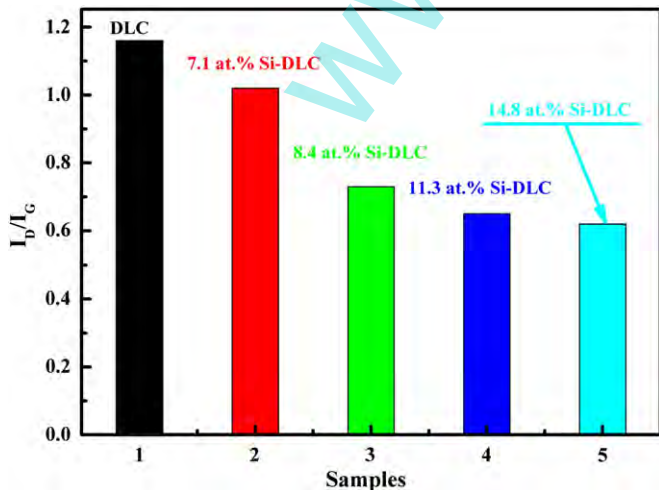


Fig. 6. Intensity ratio of the G and D peaks as a function of Si concentration.

Table 2
Atomic concentrations of carbon, silicon and oxygen detected in the films.

Samples	Concentration (at.%)			Binding energy(eV)/FWHM of C1s			
	C	Si	O	C-Si	C = C	C-C	C-O
1	92.56	—	7.44	—	284.4/1.35	284.9/1.45	286.5/1.6
2	82.34	7.14	10.52	282.9	284.2/1.35	284.7/1.45	286.5/1.6
3	80.95	8.41	10.63	283.0	284.3/1.35	284.8/1.45	286.3/1.6
4	78.08	11.26	10.66	282.9	284.2/1.35	284.7/1.45	286.5/1.6
5	74.49	14.79	10.73	283.0	284.2/1.35	284.7/1.45	286.6/1.6

than 1/10 of film thickness, which corresponds to about 300 nm, so the observed hardness reflects the actual hardness of DLC itself with the slight effect of the substrate material. It is observed that the hardness of pure DLC film is about 12.2 GPa. As the concentration of Si increases, the hardness decreases firstly and then increases. However, the C-C sp^3 and Si-C increase all along according to XPS results. At a first glance, these results are surprising and contradict each other. The above contradiction results can be explained if one considers that films prepared at by this technique are affected by colliding particles' energy. Comparing the particles' energy for low Si content Si-DLC and high Si content Si-DLC, particles during the growth of low Si content Si-DLC may have more energy than high Si content condition (it will be discussed in residual stress section). Highly energetic ion bombardment can destroy the microstructure of the DLC films and produce numerous defects, which reduces the hardness of the film. The effects of

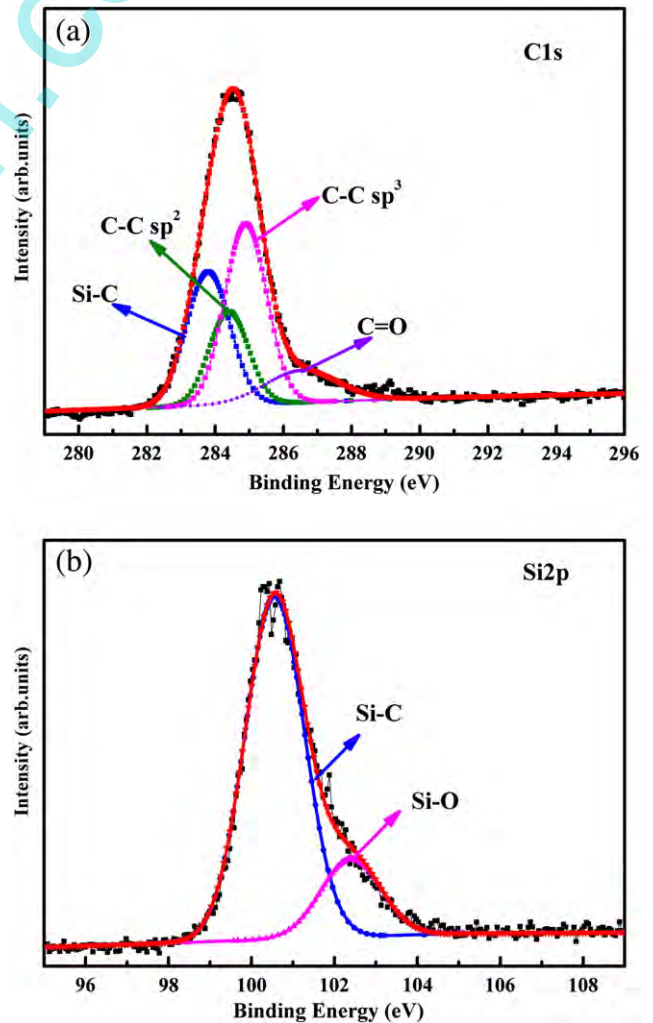


Fig. 7. Deconvoluted C1s (a) and (b) Si 2p XPS peaks for the 14.7 at.% Si-DLC film.

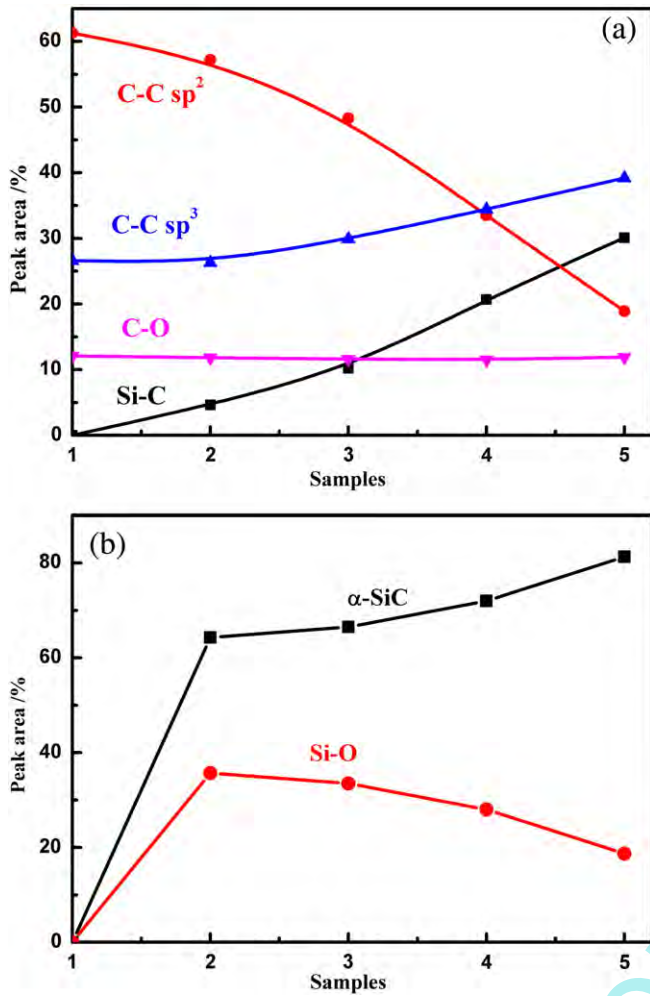


Fig. 8. The fitted peak area as a function of Si concentration. (a) From C1s and (b) Si 2p.

the ion bombardment get smaller when the Si content increases, and more sp³ C and Si-C lead to a notable increase of hardness. Thus, the alteration of colliding particles' energy works well enough to explain the changes of films hardness.

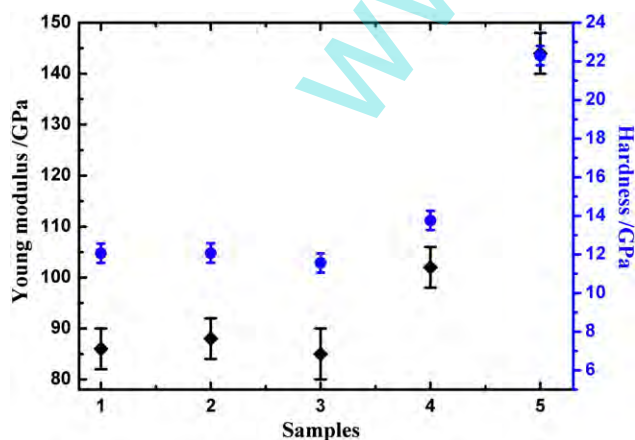


Fig. 9. Hardness and Young modulus as a function of composition. Reported values and error bars represent averages and standard deviations, respectively, based on at least three different measurements on each of as-prepared films.

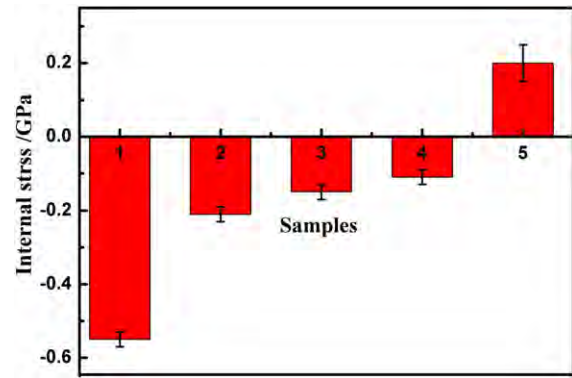


Fig. 10. Internal stress as a function of Si concentration. Reported values and error bars represent averages and standard deviations, respectively, based on at least three different measurements on each of as-prepared films.

The internal stress of Si-DLC films depends strongly on the Si concentration. The internal stress decreases monotonically with the Si concentration from 0 at.% to 14.79 at.%, as shown in Fig. 10. Comparing the stress values obtained for pure DLC and Si-DLC with 13 at.% Si, an internal stress reduction larger than three-fold is achieved. In this way, films with internal stresses lower than 0.15 GPa could be obtained. These results are attributed to the Si-C formation, confirmed by XPS results. Because the difference in the bond length between Si-C (1.89 Å) and C-C (1.54 Å) can relieve stress in a longer-range order [31]. From Fig. 10, it also note that the tensile stress is observed when 14.79 at.% Si is incorporated into DLC film, suggesting the stress state can be controlled by choosing Si concentration. Y. Pauleau [32] suggested that tensile internal stress developed in films produced from nonenergetic particles. On the contrary, compressive internal stresses developed in films produced from energetic particles. In this study, the deposition parameters are constant except SiH₄ flow. So following explanation may be a reason for the above results. When SiH₄ flow is 100 sccm, it becomes too large to be completely decomposed, resulting in the increase in nonenergetic particles. So the tensile internal stress is obtained finally.

The low COF of the DLC film plays a vital role for its industrial application. The tribological behavior of the DLC films strongly depends both on the nature of film and the testing condition. Reciprocating tribological tests have been systematically performed on the DLC and Si-DLC films under loading conditions of 10 N with ϕ 6 mm GCr 15 steel balls. The frequency is 5 Hz, and the sliding distance is

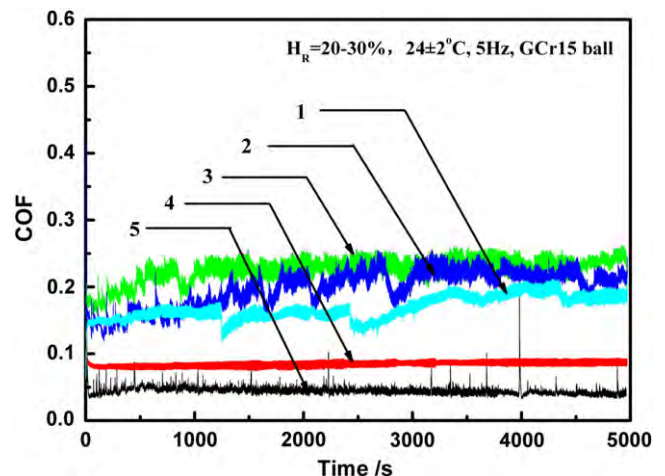


Fig. 11. Friction behavior of Si-DLC films with different Si concentration obtained with a GCr15 ball of 6 mm diameter at a sliding frequency of 5 Hz and a 10-N load under room temperature of 24 ± 2 °C and a relative humidity of 20%–30%.

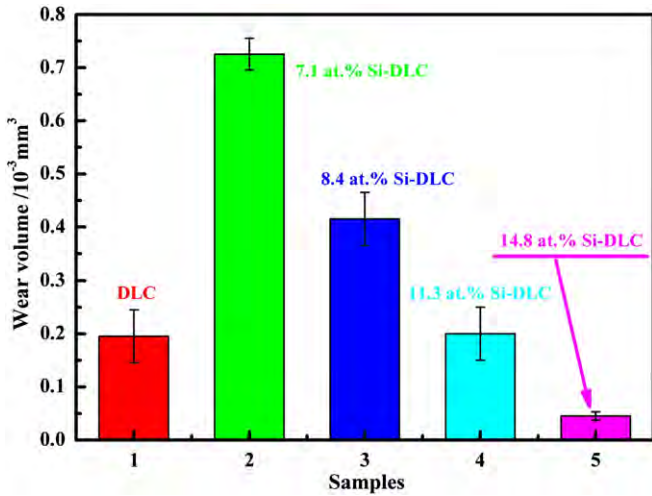


Fig. 12. Wear volume of Si-DLC film with different Si concentration in ambient air environment. Reported values and error bars represent averages and standard deviations, respectively, based on at least three different measurements on each of prepared films.

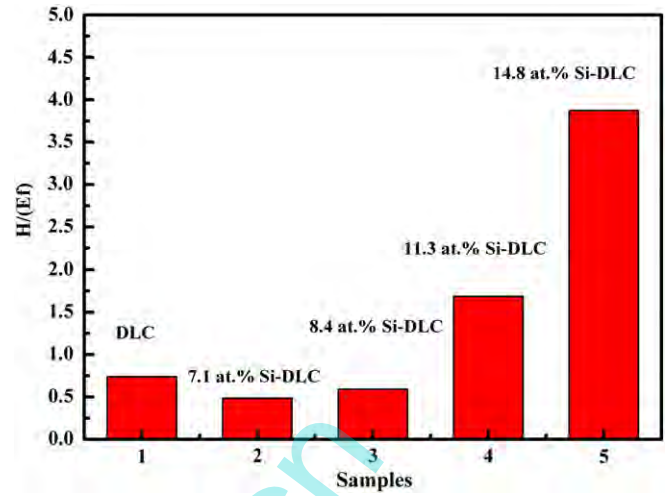


Fig. 14. $H/(Ef)$ values of Si-DLC films with different Si content.

5 mm. The representative graphs of the COF versus running time are shown in Fig. 11. For pure DLC films, the COF fluctuate from 0.15 to 0.20 with the testing time. This observation agrees with the environmental dependence of the tribological properties of pure DLC films. The friction behaviors of the Si-DLC films can be divided into two regions, the low Si content and high Si content regions, and the boundary of the two regions lies in between 8.41 and 11.26 at.% Si. With increasing Si content up to 8.41 at.%, the COF of Si-DLC film became more unstable and higher. The maximum COF of the Si-DLC film is about 0.24. The COF decreases rapidly when Si concentration is 11.24 at.%, average COF of 11.24 at.% Si-DLC is only about 0.08. Moreover, the friction behavior is quite stable. The mean COF is above 0.04 as the Si concentration goes on increase to 14.78 at.%, much lower than that of the other Si-DLC films, but sudden rises in COF are observed. It has reported that the COF between a steel ball and a DLC film is relatively high in ambient environment, ranging from 0.1 to 0.4 [33]. A major decrease in the COF appears when Si concentration over 11.26 at.%. This result means that adding Si into DLC film reduce the COF only when the content of Si increases to a certain value. Kim etc. [34] reported that the low friction behavior of Si-DLC films in air is associated with the sliding between hydrated silica debris on both track and scar surfaces. The transfer of the debris to the scar surface was observed when the silicon concentration was high. So the formation of stable oxide layer is probably the reasons for low friction. When low Si incorporates into DLC film, there is probably not enough SiO_2 formation to decrease the COF. But in the high Si content, enough SiO_2 can be formatted to decrease the COF. Sudden rises in COF (14.78 at.% Si Si-DLC) may due to the thickness of formed silicon-rich oxide debris between

the ball and the film. Once the silicon-rich oxide debris become thinner with sliding until full broke down, leading to a sudden rise in the COF. However, sliding at a higher COF would generate more debris. Thereafter, a new cycle of the dynamic friction process repeat again and again.

Effects are made to measure the wear rate of different films after tribological tests. A non-contact 3D surface profiler is used to capture 3D images on a wear track for measuring the wear volume. The wear volume of all the films is summarized in Fig. 12. It is found that the Si concentration dramatically affects the wear properties of the Si-DLC films. The wear volume of Si-DLC films increases at the beginning and then decreases with increased Si concentration. The wear volume of 7.14 at.% Si-DLC is $7.3 \times 10^{-4} \text{ mm}^3$, which is about four orders of magnitudes higher than that of the pure DLC film ($1.8 \times 10^{-4} \text{ mm}^3$). The lowest wear volume of $0.4 \times 10^{-4} \text{ mm}^3$ is achieved on the Si-DLC film with 14.79 at.% Si concentration. The wear tracks morphologies of the Si-DLC films with different concentration as shown in Fig. 13. The wear track of pure DLC seems to show small pieces of film being peeled off the substrate on random delaminated micro-regions. The low Si incorporate into DLC films lead to more large film peeled off the substrate. However, non-delaminated films are generated on the 14.79 at.% Si-DLC film surface, resulting the lowest wear rate. It is well known that the mechanical properties of films affect the wear behavior. Leyland and Matthews [35] suggested that the anti-wear is related to H/E value, where H is the hardness and E is the elastic modulus of the coating. Neuville [30] suggested that criterion H/fE will be well predicting the anti-wear results almost all coating materials, where f is the friction coefficient. In this work, the change of $H/(Ef)$ trends is close accord with that of anti-wear trends. From Fig. 14, it can be see that the $H/(Ef)$ value of Si-DLC films decreases at the beginning and then

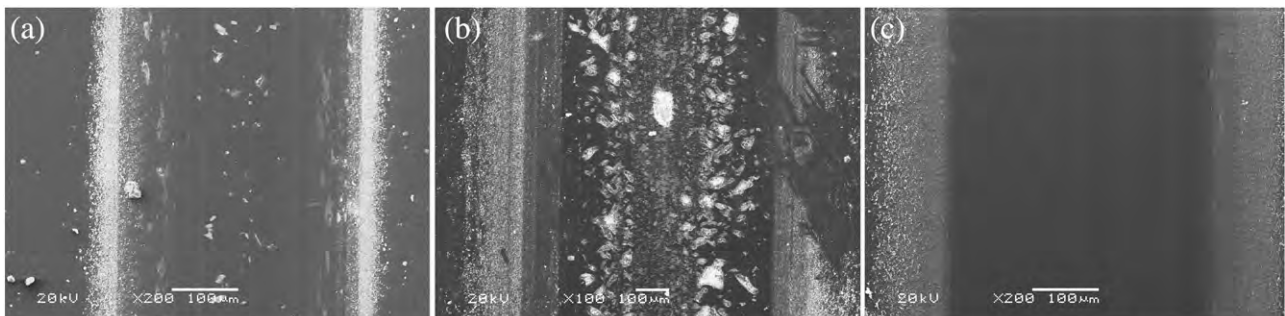


Fig. 13. SEM surface morphologies on worn track with different Si content. (a) Pure DLC, (b) Si-DLC film with 7.14 at.% Si and (c) Si-DLC film with 14.79 at.% Si.

increases with increased Si concentration. Therefore, anti-wear properties of as-prepared Si-DLC film may related to their $H/(Ef)$ ratio their $H/(Ef)$ ratio.

4. Conclusion

Si-DLC film was prepared by HCPIII method, using mixtures of C_2H_2 , Ar and diluted SiH_4 (SiH_4/Ar 10:90). Compositional and structural characterization was performed by means of Raman spectrometry and XPS. The mechanical properties and friction behavior in atmosphere environment was investigated by nanomechanical measurements and ball-on-disc tribometer, respectively. The major results are drawn as follows:

- (1) The composition of the Si-DLC films can be controlled by changing the flow rate of C_2H_2 and SiH_4 gas in the HCPIII deposition process. The average grain size for the film surface morphology is decreased along with the increased of Si concentration. But at the same time, the root mean square values are increased.
- (2) Both the hardness and elastic modulus suffer degradation when the silicon concentration is low, but these properties recover when Si concentration increase. This is probably caused by the variation of colliding particles' energy. The Si-DLC film with tensile stress and compressive stress can be obtained by choosing distinct contents of Si in the film.
- (3) The addition of Si into DLC film reduces the COF and wear rate only when content of Si increases to a certain value. The formation of stable oxide layer on Si-DLC films is one of the reasons for the low friction. The different $H/(Ef)$ ratio are determined to be the basis for the changes in wear rate.

Acknowledgment

The authors are grateful for financial support from the National Natural Science Foundation of China (grant no. 11172300).

References

- [1] C. Donnet, Surf. Coat. Technol. 100–101 (1998) 180–186.
- [2] J. Robertson, Mater. Sci. Eng., R Rep. 37 (2002) 129–281.
- [3] R.K. Roy, K.-R. Lee, J. Biomed. Mater. Res. B Appl. Biomater. 83B (2007) 72–84.
- [4] M. Sedlaček, B. Podgornik, J. Vižintin, Mater. Charact. 59 (2008) 151–161.
- [5] S. Sattel, J. Robertson, H. Ehrhardt, J. Appl. Phys. 82 (1997) 4566–4576.
- [6] R. Hatada, S. Flege, K. Baba, W. Ensinger, H.J. Kleebe, I. Sethmann, S. Lauterbach, J. Appl. Phys. 107 (2010), (083307-083307-083306).
- [7] H. Li, T. Xu, C. Wang, J. Chen, H. Zhou, H. Liu, Appl. Surf. Sci. 249 (2005) 257–265.
- [8] X. Liu, J. Yang, J. Hao, J. Zheng, Q. Gong, W. Liu, Adv. Mater. 24 (2012) 4614–4617.
- [9] O. Wilhelmsson, M. Räsander, M. Carlsson, E. Lewin, B. Sanyal, U. Wiklund, O. Eriksson, U. Jansson, Adv. Funct. Mater. 17 (2007) 1611–1616.
- [10] S. Zhou, L. Wang, Z. Lu, Q. Ding, S.C. Wang, R.J. Wood, Q. Xue, J. Mater. Chem. 22 (2012) 15782–15792.
- [11] T. Iseki, H. Mori, H. Hasegawa, H. Tachikawa, K. Nakanishi, Diamond Relat. Mater. 15 (2006) 1004–1010.
- [12] M. Vila, J.M. Carrapichano, J.R. Gomes, S.S. Camargo Jr., C.A. Achete, R.F. Silva, Wear 265 (2008) 940–944.
- [13] K.-R. Lee, M.-G. Kim, S.-J. Cho, K. Yong Eun, T.-Y. Seong, Thin Solid Films 308–309 (1997) 263–267.
- [14] P. Papakonstantinou, J.F. Zhao, P. Lemoine, E.T. McAdams, J.A. McLaughlin, Diamond Relat. Mater. 11 (2002) 1074–1080.
- [15] A. Bendavid, P.J. Martin, C. Comte, E.W. Preston, A.J. Haq, F.S. Magdon Ismail, R.K. Singh, Diamond Relat. Mater. 16 (2007) 1616–1622.
- [16] S. Fujimoto, N. Ohtake, O. Takai, Surf. Coat. Technol. 206 (2011) 1011–1015.
- [17] Y. Wang, L. Wang, G. Zhang, S.C. Wang, R.J.K. Wood, Q. Xue, Surf. Coat. Technol. 205 (2010) 793–800.
- [18] H. Cho, S. Kim, H. Ki, Acta Mater. 60 (2012) 6237–6246.
- [19] T. Kitagawa, I. Yamada, N. Toyoda, H. Tsubakino, J. Matsuo, G.H. Takaoka, A. Kirkpatrick, Nucl. Instrum. Methods Phys. Res. B 201 (2003) 405–412.
- [20] A. Soum-Glaude, G. Rambaud, S.E. Grillo, L. Thomas, Thin Solid Films 519 (2010) 1266–1271.
- [21] H. Liu, Q. Xu, C. Wang, X. Zhang, B. Tang, Surf. Coat. Technol. 228 (2013) 159–163.
- [22] J.L. Endrino, R. Escobar Galindo, H.S. Zhang, M. Allen, R. Gago, A. Espinosa, A. Anders, Surf. Coat. Technol. 202 (2008) 3675–3682.
- [23] J. Wang, J. Pu, G. Zhang, L. Wang, ACS Appl. Mater. Interfaces 5 (2013) 5015–5024.
- [24] S. Neuville, A. Matthews, Thin Solid Films 515 (2007) 6619–6653.
- [25] F.C. Tai, S.C. Lee, J. Chen, C. Wei, S.H. Chang, J. Raman Spectrosc. 40 (2009) 1055–1059.
- [26] F.C. Tai, S.C. Lee, C.H. Wei, S.L. Tyan, Mater. Trans. 47 (2006) 6.
- [27] C. Casiraghi, A.C. Ferrari, J. Robertson, Phys. Rev. B 72 (2005) 085401.
- [28] C. Cao, H. Zhu, H. Wang, Thin Solid Films 368 (2000) 203–207.
- [29] W.Y. Lee, J. Appl. Phys. 51 (1980) 3365–3372.
- [30] S. Neuville, Surf. Coat. Technol. 206 (2011) 703–726.
- [31] T. Takeshita, Y. Kurata, S. Hasegawa, J. Appl. Phys. 71 (1992) 5395–5400.
- [32] Y. Pauleau, Vacuum 61 (2001) 175–181.
- [33] R. Memming, H. Tolle, P. Wierenga, Thin Solid Films 143 (1986) 31–41.
- [34] M.-G. Kim, K.-R. Lee, K.Y. Eun, Surf. Coat. Technol. 112 (1999) 204–209.
- [35] A. Leyland, A. Matthews, Wear 246 (2000) 1–11.